Hybrid Control for a Boost DC-DC Converter With Average Dwell Time

Seyed Hamed Hashemi
Department of Electrical Engineering, Faculty of Engineering
Ferdowsi University of Mashhad (FUM)
Mashhad, Iran
Hamedhashemi1371@gmail.com

Naser Pariz
Department of Electrical Engineering, Faculty of Engineering
Ferdowsi University of Mashhad (FUM)
Mashhad, Iran
n-pariz@um.ac.ir

***Abstract*—This paper peruses the voltage control of a boost DC-DC converter. The hybrid model of the converter is utilized to introduce a new switching control law, which regulates the output voltage of the converter. In this switching control law an average dwell time constraint is considered. This suggestion guarantees the exponential stability of a desired output voltage value. Furthermore, in the proposed switching control law, there exist no Zeno solutions, since the existence of the average dwell time constraint. Moreover, in power converters, two significant concerns are switching loss and electromagnetic interference resulting from numerous rates of variations of voltage and current. Therefore, the salient features of the proposed controller are the mitigation of the switching rate as well as the regulation of the output voltage. Finally, simulation experiments are followed through on a boost converter to validate the effectiveness and superiority of the proposed control strategy.**

Keywords*—Switched linear systems, Boost DC-DC converters, Average dwell time.

I. Introduction

The boost DC-DC converter is the most popular converter in energy conversion systems, due to its lightweight, compact size, high efficiency, and reliability. Thereafter, a large number of research works were focused on the improvement of controllers for the converter [1]. The main purpose of presented controllers is to regulate the output voltage to track the desired value in the presence of the load and voltage source disturbances [2]. Therefore, this paper presents a switching control law to accomplish this task.

There are different types of models for the converter, which can be classified into two categories; the average model, and the hybrid model. Most of the provided methods were based on the average model because of its simplicity. For example, in [3], based on the average model of the converter, a LQR controller was designed to adjust the output voltage. Besides, in [4] an adaptive sliding mode controller was presented to control the output voltage, and reject disturbances. Neural network-based controller [5], fuzzy logic [6], and the combination of these two methods were utilized to control the converter [7]. The proportional integral derivative (PID) controller is one of the popular control technique that has been extensively used to control the boost converter [8], [9], because of its simple control construction and design procedure. Nonetheless, in the highly nonlinear and uncertain systems, its performance is not acceptable. In [10] sliding surface was utilized to design a robust controller, nevertheless, this controller suffers from problems associated with the average model. In the average model, the switch, the capacitor and inductor are considered ideal, and the equivalent series resistance (ESR) is neglected. Furthermore, the accuracy of the average model depends on the separation of time scales [11]. The robustness and dynamic performance analysis based on the average model have not yet been articulated [12].

The other model for the boost converter is the hybrid model. In this model, based on states of the switch, four modes are considered [13]. Since the hybrid model is superior to the average model, controllers based on this scheme have gained attention. In [14], a reference voltage and a reference current were calculated by the energy balance principle to introduce a new switching control law. Based on the optimal control theory and N-step model, a controller was presented for the converter [15]. In [16], to minimize the cosine of the angle between regulation error and vector field, the new switching low was defined. A sliding mode controller was presented in [17] to control the output voltage. Nevertheless, it was only employed for converter operating in Continuous Current Mode (CCM). Furthermore, Mixed-Integer Quadratic Programming (MIQP) was studied in [18] to address the reference tracking and the regulation problem, which could provide the operation of the converter in both continuous and discontinuous current modes. The other technique to regulate the output voltage was presented in [19], where new transition conditions for both continuous and discontinuous current modes were defined. In [20], different control procedures were compared through experimentation for the Buck and boost converters. In [21], based on the Lyapunov function, a state-dependent switching law was introduced. This method guaranteed robust global asymptotic stability of a desired output voltage value. Nevertheless, when the spatial regularization parameter is zero, this controller can be shown to be unable to achieve exponential stability, which is the main shortcoming of this method.

Moreover, it is crucial in power converters to have low switching frequency, because of the switching loss and electromagnetic interference. Accordingly, this paper introduces a switching control law in which an average dwell time constraint is considered. Since the average dwell time is more

978-0-7381-1197-1/21/$31.00 ©2021 IEEE

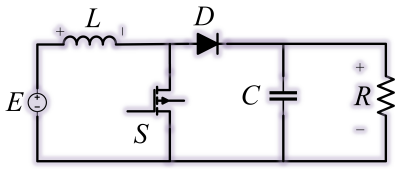

Fig. 1. Schematic diagram of a boost DC-DC converter.

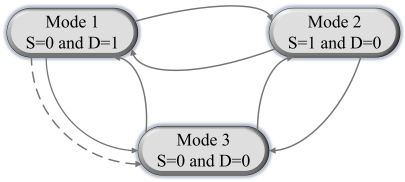

Fig. 2. A hybrid automaton scheme of a boost converter.

TABLE I
TRANSITION CONDITIONS [13].

$Transition$ $Mode() \rightarrow Mode()$	$Guard$	$Reset$
$1 \rightarrow 2$	$S = 1$ *and* $V_c \geq 0$	
$1 \rightarrow 3$	$i_L = 0$ *and* $V_c \geq E$	
$1 \Rightarrow 3$	$i_L < 0$	$i_L^+ = 0$
$1 \rightarrow 4$	$S = 1$ *and* $V_c \leq 0$	$V_c^+ = 0$
$2 \rightarrow 1$	$S = 0$ *and* $i_L \geq 0$	
$2 \rightarrow 3$	$S = 0$ *and* $i_L \leq 0$	$i_L^+ = 0$
$2 \rightarrow 4$	$V_c = 0$	
$2 \Rightarrow 4$	$V_c < 0$	$V_c^+ = 0$
$3 \rightarrow 1$	$V_c = E$	
$3 \rightarrow 2$	$S = 1$ *and* $V_c \geq 0$	
$3 \rightarrow 4$	$S = 1$ *and* $V_c \leq 0$	$V_c^+ = 0$
$4 \rightarrow 1$	$S = 0$ *and* $i_L \geq 0$	
$4 \rightarrow 3$	$S = 0$ *and* $i_L \leq 0$	$i_L^+ = 0$
$4 \Rightarrow 4$	$V_c < 0$	$V_c^+ = 0$

flexible than the dwell time method, therefore, it became a popular technique for stabilization of switched systems [22]. The switched system is exponentially stable if the number of switches in the finite time interval is limited, and the average time between consecutive switching is greater than or equal to a positive constant [23], [24]. Therefore, this paper presents a switching control law to guarantee the exponential stability of a desired output voltage value. In this switching control law, an average dwell time constraint is considered with the switching control law. The low switching frequency and exponential stability are the salient features of this strategy, which are confirmed and validated via simulations.

The remainder of this paper is organized as follows. In section (2), the hybrid model of the converter is investigated. The proposed switching control law is introduced in section (3). Simulation results are shown in section (4). Finally, concluding remarks are presented in Section (5).

II. HYBRID MODELING AND AUTOMATON EXHIBITION

The boost DC-DC converter (Fig. 1) consists of a capacitor (C), a Diode (D), a voltage source (E), an inductor (L), a load (R), and an insulated gate bipolar transistor (S). The existence of switching elements (D and S) yields a hybrid system. The task of a boost converter is to step up the voltage source (E). Four modes can be considered for the converter based on the states of switches (ON, OFF); (D=ON, S=OFF), (D=OFF, S=ON), (D=OFF, S=OFF), (D=ON, S=ON). Fig. 2 demonstrates a hybrid automaton representation of the converter. Mode 4 is emitted since it is not feasible. In mode 1, the switch is off (S=0), and the diode is conducting, so the inductor current starts reducing, and the capacitor charge starts growing. When the switch is on (S=1), and the diode is off (D=0), the inductor current starts increasing, and the capacitor supports the load, this is mode 2. In mode 3, both the switch and diode are off (S=0, D=0). When the converter operates in this mode, the inductor current reaches zero and it is said that the converter operates in Discontinuous Current Mode (DCM). Mode 4 is not a feasible state and cannot occur when the converter is working. The transition conditions are summarized in Table I [13]. The differential equations for each mode based on the specific values of the S and D are expressed as follows.

$$
\begin{aligned}
Mode \quad 1 &: \begin{cases} S = 0 \\ D = 1 \\ \dot{V}_c = \frac{-V_c}{RC} + \frac{i_L}{C} \\ \dot{i}_L = \frac{-V_c}{L} + \frac{E}{L} \end{cases} \qquad
Mode \quad 2 : \begin{cases} S = 1 \\ D = 0 \\ \dot{V}_c = \frac{-V_c}{RC} \\ \dot{i}_L = \frac{E}{L} \end{cases} \\
Mode \quad 3 &: \begin{cases} S = 0 \\ D = 0 \\ \dot{V}_c = \frac{-V_c}{RC} \\ \dot{i}_L = 0 \end{cases} \qquad
Mode \quad 4 : \begin{cases} S = 1 \\ D = 1 \\ \dot{V}_c = 0 \\ \dot{i}_L = \frac{E}{L} \end{cases}
\end{aligned} \tag{1}
$$

By utilizing the Krasovskii regularization, a switched differential inclusion which contains all possible modes can be defined as follows. For details, see [21].

$$
\dot{x} \in F_S(x), \ x \in \tilde{M}_S := \begin{cases} \tilde{M}_0 = \{x \in \mathbb{R}^2 : i_L \geq 0\} \\ \tilde{M}_1 = \{x \in \mathbb{R}^2 : V_c \geq 0\} \end{cases} \tag{2}
$$

In (2), $x = [V_c \quad i_L]^T$ is the state vector, and $\tilde{M}_s$ are the sets that capture the regions of validity for each mode. Therefore, the differential equations expressing the boost converter can be represented as a differential inclusion as follows.

$$
\begin{aligned}
F_0(x) &= \begin{cases} \left\{ \begin{bmatrix} \frac{-V_c}{RC} + \frac{i_L}{C} \\ \frac{-V_c}{L} + \frac{E}{L} \end{bmatrix} \right\}, & \text{if } x \in \bar{M}_1 \backslash \bar{M}_2 \\ \left\{ \frac{-V_c}{RC} \right\} \times \left[\frac{-V_c}{L} + \frac{E}{L} \ \ 0 \right], & \text{if } x \in \bar{M}_2 \end{cases} \\
F_1(x) &= \begin{bmatrix} \frac{-V_c}{RC} \\ \frac{E}{L} \end{bmatrix}, \quad \text{if } x \in \tilde{M}_1
\end{aligned} \tag{3}
$$

In (3), the sets $\bar{M}_1$, $\bar{M}_2$ are given as follows.

$$
\begin{aligned}
\bar{M}_1 &= \{x \in \mathbb{R}^2 : i_L > 0\} \cup \{x \in \mathbb{R}^2 : V_c \leq E, \ i_L = 0\} \\
\bar{M}_2 &= \{x \in \mathbb{R}^2 : V_c > E, \ i_L = 0\}
\end{aligned} \tag{4}
$$

III. PROPOSED SWITCHING CONTROL LAW

The control objective is to adjust the output voltage to track a constant desired value. Thereafter, the following Lyapunov

function candidate is used to introduced the proposed switching technique.

$$V(x) = (x - x^*)^T P(x - x^*), \quad P = \begin{bmatrix} p_{11} & 0 \\ 0 & p_{22} \end{bmatrix} \tag{5}$$

Where x^* is the desired state, and P is a symmetric positive definite matrix. Based on the Lyapunov function and its gradient, the following switching law, which works instead of the pulse width modulation (PWM), has been presented [21].

$$\begin{aligned}
&S = \underset{S' \in \{0,1\}}{\arg\min} \ \max_{\xi \in F_{S'}(x)} \langle \nabla V(x), \xi \rangle , \\
&\max_{\xi \in F_{S'}(x)} \langle \nabla V(x), \xi \rangle \ = \begin{cases} \tilde{\gamma}_0(x) & \text{if } S' = 0 \\ \tilde{\gamma}_1(x) & \text{if } S' = 1 \end{cases} \\
&\tilde{\gamma}_0(x) = 2p_{11}(V_c - V_c^*)(\frac{-V_c}{RC} + \frac{i_L}{C}) + 2p_{22}(i_L - i_L^*) \\
&(\frac{-V_c + E}{L}) + K_0(V_c - V_c^*)^2, \ \tilde{\gamma}_1(x) = \frac{-2V_c p_{11}(V_c - V_c^*)}{RC} \\
&+ \frac{2Ep_{22}(i_L - i_L^*)}{L} + K_1(V_c - V_c^*)^2, \ p_{11} = \frac{C}{2}, \ p_{22} = \frac{L}{2}
\end{aligned} \tag{6}$$

Where K_0, K_1 are design parameters, and i_L^*, V_c^* are desired values. Accordingly, the following hybrid system has been introduced.

$$\begin{aligned}
&\begin{bmatrix} \dot{x} \\ \dot{S} \end{bmatrix} \in \begin{bmatrix} F_S(x) \\ 0 \end{bmatrix}, \quad \begin{matrix} (x,S) \in C = \{(x,S) : x \in \tilde{M}_0, \tilde{\gamma}_0 \le 0, \\ S = 0\} \cup \{(x,S) : x \in \tilde{M}_1, \tilde{\gamma}_1 \le 0, S = 1\} \end{matrix} \\
&\begin{bmatrix} x^+ \\ S^+ \end{bmatrix} \in \begin{bmatrix} x \\ G(x) \end{bmatrix}, \quad \begin{matrix} (x,S) \in D = \{(x,S) : x \in \tilde{M}_0, \tilde{\gamma}_0 = 0, \\ S = 0\} \cup \{(x,S) : x \in \tilde{M}_1, \tilde{\gamma}_1 = 0, S = 1\} \end{matrix} \\
&G(x) = \begin{cases} \{1\} \text{ if } S = 0 \\ \{0\} \text{ if } S = 1 \end{cases}
\end{aligned} \tag{7}$$

The main limitation of the above switching law is the Zeno solutions near the operating point. The authors in [21] suggested increasing the spatial regularization parameter to suppress the Zeno solutions. Nevertheless, this paper suggests considering an average dwell time constraint with the switching law to solve this problem. Moreover, this suggestion guarantees the exponential stability of the desired voltage.

Definition [23]: Consider a switching signal $\sigma(t)$, and a time interval $0 \le t_1 \le t_2$, which has $N_\sigma(t_1, t_2)$ number of discontinuities. Therefore, N_0 and τ are called the chatter bound, and the average dwell time, respectively, if the following condition holds for $N_0 \ge 1$, and $\tau > 0$.

$$N_\sigma(t_1, t_2) \le N_0 + \frac{t_2 - t_1}{\tau}, \quad \forall t_2 \ge t_1 \ge 0 \tag{8}$$

Theorem: Consider the continuous-time switched linear system $\dot{x}(t) = A_i x(t), \ i \in \{1, \cdots, M\}$. Given positive constants $\delta_1 > 0$, $\delta_2 > 0$, $\lambda \ge 0$, and a symmetric positive definite matrix P. Suppose there exists a continuously differentiable function $V(x(t)) : \mathbb{R}^2 \to \mathbb{R}$ such that

$$V(x) = x^T P x, \ \begin{cases} \delta_1 \|x(t)\|^2 \le V(x(t)) \le \delta_2 \|x(t)\|^2 & (a) \\ \dot{V}(x(t)) \le -\lambda V(x(t)) & (b) \end{cases} \tag{9}$$

thereafter, the system is uniformly exponentially stable under any switching signal with average dwell time

$$\tau > \frac{1}{\lambda}(\ln \delta_2 - \ln \delta_1). \tag{10}$$

Where M is the number of subsystems.

Proof: Taking integration of (9b) over the interval $[t \ t_k)$, it follows that

$$V(x(t)) \le e^{-\lambda(t - t_k)} V(x(t_k)). \tag{11}$$

From (11), provided that

$$V(x(t_{k+1})) \le e^{-\lambda(t_{k+1} - t_k)} V(x(t_k)). \tag{12}$$

From (9a) it can be concluded that

$$\delta_1 \|x(t_{k+1})\|^2 \le V(x(t_{k+1})), \ V(x(t_k)) \le \delta_2 \|x(t_k)\|^2. \tag{13}$$

Then, it follows from (12) and (13)

$$\delta_1 \|x(t_{k+1})\|^2 \le e^{-\lambda(t_{k+1} - t_k)} \delta_2 \|x(t_k)\|^2. \tag{14}$$

Letting $\delta_2/\delta_1 = \mu$, (14) can be rewritten as follows.

$$\|x(t_{k+1})\|^2 \le \mu e^{-\lambda(t_{k+1} - t_k)} \|x(t_k)\|^2 \tag{15}$$

The time progression of (15) is determined as follows.

$$\begin{aligned}
&\|x(t_{k+1})\|^2 \le \mu e^{-\lambda(t_{k+1} - t_k)} \|x(t_k)\|^2, \\
&\|x(t_k)\|^2 \le \mu e^{-\lambda(t_k - t_{k-1})} \|x(t_{k-1})\|^2 \\
&\Rightarrow \|x(t_{k+1})\|^2 \le \mu^2 e^{-\lambda(t_{k+1} - t_{k-1})} \|x(t_{k-1})\|^2, \\
&\|x(t_{k-1})\|^2 \le \mu e^{-\lambda(t_{k-1} - t_{k-2})} \|x(t_{k-2})\|^2 \\
&\Rightarrow \|x(t_{k+1})\|^2 \le \mu^3 e^{-\lambda(t_{k+1} - t_{k-2})} \|x(t_{k-2})\|^2, \ \cdots \\
&\|x(t_{k+1})\|^2 \le \mu^{N_\sigma + 1} e^{-\lambda(t_{k+1} - t_0)} \|x(t_0)\|^2, \\
&t_0 = 0, \ t_{k+1} = T, \Rightarrow \|x(t_{k+1})\|^2 \le \mu^{N_0 + 1 + \frac{T}{\tau}} e^{-\lambda T} \|x(t_0)\|^2 \\
&= \|x(t_{k+1})\|^2 \le e^{(N_0 + 1 + \frac{T}{\tau}) \ln \mu} e^{-\lambda T} \|x(t_0)\|^2 \\
&= \|x(t_{k+1})\|^2 \le e^{(N_0 + 1) \ln \mu} e^{(\frac{\ln \mu}{\tau} - \lambda) T} \|x(t_0)\|^2 \\
&\Rightarrow \|x(t_{k+1})\| \le e^{\frac{1}{2}(N_0 + 1) \ln \mu} e^{(\frac{\ln \mu}{\tau} - \lambda) T} \|x(t_0)\|
\end{aligned} \tag{16}$$

With the condition of (10), one can straightway realize

$$\frac{\ln \mu}{\tau} - \lambda \le 0 \Rightarrow \frac{\ln \mu}{\lambda} \le \tau \Rightarrow \tau \ge \frac{1}{\lambda}(\ln \delta_2 - \ln \delta_1). \tag{17}$$

Therefore, it can be deduced that $V(x)$ exponentially converges to zero as $t \to \infty$, if the average dwell time satisfies (10). □

Finally, the proposed hybrid system is introduced as follows, which contains the augmented variable (sampling timer). This variable enumerates down up to it attains zero. At this point, it resets to the average dwell time τ.

$$\begin{aligned}
&\begin{bmatrix} \dot{x} \\ \dot{S} \end{bmatrix} \in \begin{bmatrix} F_S(x) \\ -1 \\ 0 \end{bmatrix}, \quad (x,S) \in C \times [0 \quad \tau] \\
&\begin{bmatrix} x^+ \\ S^+ \end{bmatrix} = \begin{bmatrix} x \\ \tau \\ G(x) \end{bmatrix}, \quad (x,S) \in D \times \{0\}
\end{aligned} \tag{18}$$

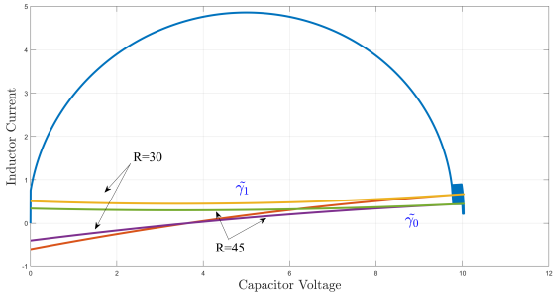

Fig. 3. Phase plane path and the switching surface for the first experiment.

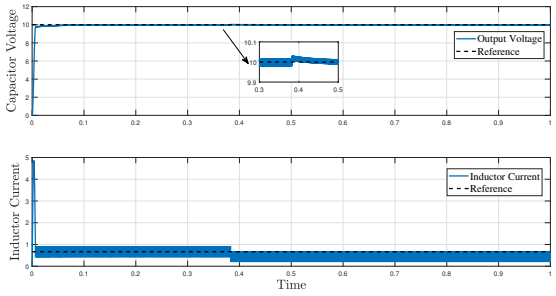

Fig. 4. Plot of output voltage and inductor current versus time for the first experiment.

IV. Numerical Validation

In order to further investigate the performance of the proposed switching control law, two experiments are performed. In the first experiment, a variation in load resistance is considered to peruse the robustness of the proposed controller. In the second experiment, the desired output voltage value is changed to study the performance of the proposed controller. As mentioned above, this paper suggests considering an average dwell time constraint with the switching control law to avoid the Zeno solutions. This suggestion decreases the switching frequency and guarantees the exponential stability. HyEQ toolbox [25] is used to perform the simulations.

A. First experiment

The boost converter parameters for this trial are selected as $(E = 5V,\ C = 2000\mu F,\ L = 2200\mu H,\ R = 30\Omega)$. According to the selection of P, the average dwell time is considered 100 microseconds, and the desired output voltage is $10V$. Moreover, the initial condition for the inductor current and capacitor voltage is (0,0). In order to show the load disturbance rejection capability of the proposed method, a step change is applied in the load. The range of the step change is identical to $\%50$ of the load resistance at the operating point, in order to create 15Ω variations in the load. The simulation results corresponding to this trial are shown in Figs. 3-5. Fig. 3 depicts switching boundaries of the proposed controller, and state trajectory. The average dwell time led to the ejection of the parabolas. The inductor current and output voltage reached and settled at the desired values quickly, which are shown in Fig. 4. This figure illustrates that the disturbance was entirely rejected by the proposed controller. Switching signal and tracking error are shown in Fig. 5. This figure shows that the steady-state error is zero, and the number of jumps is 9937.

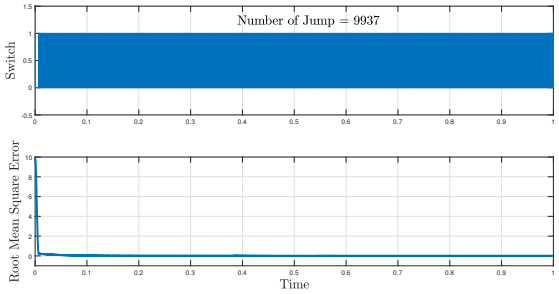

Fig. 5. Switching signal and tracking error for the first experiment.

B. Second experiment

In this experiment there is a step change in the desired output voltage, i.e., the desired output voltage value $V^* = 7V$ is varied to $8V$ at $t = 1.85sec$. For this experiment the boost converter parameters are chosen as $(E = 5V,\ C = 0.1F,\ L = 0.2H,\ R = 3\Omega)$. Moreover, the initial condition of the inductor current and capacitor voltage is (5,0). The simulation results of this experiment are shown in Figs. 6-8. Fig. 6 demonstrates switching boundaries of the proposed controller, and state trajectory. Fig. 7 shows the inductor current and output voltage. It can be deduced that the proposed controller regulated the output voltage to attentively track the reference voltage. Fig. 8 depicts switching signal during the time and tracking error. In this experiment, the steady-state error is zero, and the number of jumps is 9710.

The simulation results reveal the efficiency and the robustness of the proposed switching control law. Furthermore, it can be concluded that the switching frequency of the proposed technique is acceptable, which leads to suppress the switching loss and electromagnetic interference, while the steady-state error is zero,

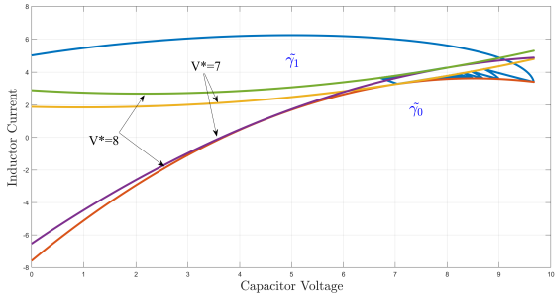

Fig. 6. Phase plane path and the switching surface for the second experiment.

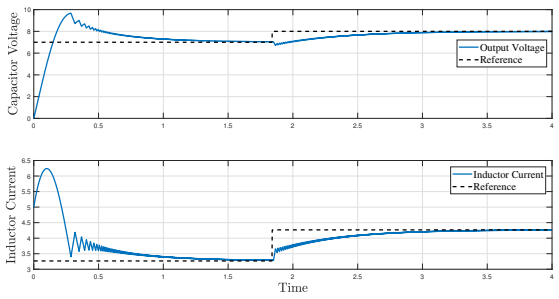

Fig. 7. Plot of output voltage and inductor current versus time for the second experiment.

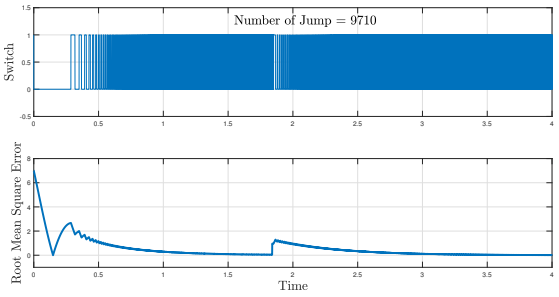

Fig. 8. Switching signal and tracing error for the second experiment.

V. Conclusion

This paper studied the voltage control of a boost converter based on the hybrid control technique. The hybrid model of the boost converter was investigated to present the new switching control law. Thereafter, it was highlighted that the main topic of the controller design for a power converter is the switching frequency. It was also mentioned that the high switching frequency causes a electromagnetic interference and switching loss. In order to solve this problem, it was suggested considering an average dwell time constraint with the switching control law. This suggestion guaranteed the exponential stability of the closed-loop system, and led to a reduction in the switching frequency. The simulation results confirmed the validity and advantage of the proposed controller.

References

[1] F. M. Oettmeier, J. Neely, S. Pekarek, R. DeCarlo, and K. Uthaichana, "Mpc of switching in a boost converter using a hybrid state model with a sliding mode observer," *IEEE Transactions on Industrial Electronics*, vol. 56, no. 9, pp. 3453–3466, 2008.

[2] O. Kirshenboim and M. M. Peretz, "Fast response of deviation-constrained hybrid controllers for indirect energy transfer converters," *IEEE Transactions on Power Electronics*, vol. 33, no. 3, pp. 2615–2629, 2017.

[3] C. Olalla, R. Leyva, A. El Aroudi, and I. Queinnec, "Robust lqr control for pwm converters: An lmi approach," *IEEE Transactions on industrial electronics*, vol. 56, no. 7, pp. 2548–2558, 2009.

[4] S. Oucheriah and L. Guo, "Pwm-based adaptive sliding-mode control for boost dc–dc converters," *IEEE Transactions on industrial electronics*, vol. 60, no. 8, pp. 3291–3294, 2012.

[5] R.-J. Wai and L.-C. Shih, "Adaptive fuzzy-neural-network design for voltage tracking control of a dc–dc boost converter," *IEEE transactions on power electronics*, vol. 27, no. 4, pp. 2104–2115, 2011.

[6] K. Mehran, D. Giaouris, and B. Zahawi, "Stability analysis and control of nonlinear phenomena in boost converters using model-based takagi–sugeno fuzzy approach," *IEEE Transactions on Circuits and Systems I: Regular Papers*, vol. 57, no. 1, pp. 200–212, 2009.

[7] R.-J. Wai, M.-W. Chen, and Y.-K. Liu, "Design of adaptive control and fuzzy neural network control for single-stage boost inverter," *IEEE Transactions on Industrial Electronics*, vol. 62, no. 9, pp. 5434–5445, 2015.

[8] M. M. Anzehaee, B. Behnam, and P. Hajihosseini, "Augmenting armarkov-pfc predictive controller with pid-type iii to improve boost converter operation," *Control Engineering Practice*, vol. 79, pp. 65–77, 2018.

[9] V. Mummadi, "Design of robust digital pid controller for h-bridge soft-switching boost converter," *IEEE Transactions on Industrial Electronics*, vol. 58, no. 7, pp. 2883–2897, 2010.

[10] O. Lopez-Santos, L. Martinez-Salamero, G. Garcia, H. Valderrama-Blavi, and T. Sierra-Polanco, "Robust sliding-mode control design for a voltage regulated quadratic boost converter," *IEEE transactions on power electronics*, vol. 30, no. 4, pp. 2313–2327, 2014.

[11] A. Ghasemian and A. Taheri, "Constrained near-time-optimal sliding-mode control of boost converters based on switched affine model analysis," *IEEE Transactions on Industrial Electronics*, vol. 65, no. 1, pp. 887–897, 2017.

[12] P. Karamanakos, T. Geyer, and S. Manias, "Direct voltage control of dc–dc boost converters using enumeration-based model predictive control," *IEEE Transactions on Power Electronics*, vol. 29, no. 2, pp. 968–978, 2013.

[13] W. Heemels, M. K. Çamlıbel, A. Van Der Schaft, and J. Schumacher, "Modelling, well-posedness, and stability of switched electrical networks," in *International Workshop on Hybrid Systems: Computation and Control*. Springer, 2003, pp. 249–266.

[14] P. Gupta and A. Patra, "Hybrid mode-switched control of dc-dc boost converter circuits," *IEEE Transactions on Circuits and Systems II: Express Briefs*, vol. 52, no. 11, pp. 734–738, 2005.

[15] T. Geyer, G. Papafotiou, and M. Morari, "On the optimal control of switch-mode dc-dc converters," in *International Workshop on Hybrid Systems: Computation and Control*. Springer, 2004, pp. 342–356.

[16] C. Sreekumar and V. Agarwal, "Hybrid control of a boost converter operating in discontinuous current mode," in *2006 37th IEEE Power Electronics Specialists Conference*. IEEE, 2006, pp. 1–6.

[17] P. Gupta and A. Patra, "Hybrid sliding mode control of dc-dc power converter circuits," in *TENCON 2003. Conference on Convergent Technologies for Asia-Pacific Region*, vol. 1. IEEE, 2003, pp. 259–263.

[18] M. Hejri and H. Mokhtari, "Hybrid predictive control of a dc–dc boost converter in both continuous and discontinuous current modes of operation," *Optimal Control Applications and Methods*, vol. 32, no. 3, pp. 270–284, 2011.

[19] C. Sreekumar and V. Agarwal, "A hybrid control algorithm for voltage regulation in dc–dc boost converter," *IEEE Transactions on Industrial Electronics*, vol. 55, no. 6, pp. 2530–2538, 2008.

[20] S. Mariéthoz, S. Almér, M. Bâja, A. G. Beccuti, D. Patino, A. Wernrud, J. Buisson, H. Cormerais, T. Geyer, H. Fujioka *et al.*, "Comparison of hybrid control techniques for buck and boost dc-dc converters," *IEEE transactions on control systems technology*, vol. 18, no. 5, pp. 1126–1145, 2009.

[21] T. A. Theunisse, J. Chai, R. G. Sanfelice, and W. M. H. Heemels, "Robust global stabilization of the dc-dc boost converter via hybrid control," *IEEE Transactions on Circuits and Systems I: Regular Papers*, vol. 62, no. 4, pp. 1052–1061, 2015.

[22] Y. Jin, Y. Zhang, Y. Jing, and J. Fu, "An average dwell-time method for fault-tolerant control of switched time-delay systems and its application," *IEEE Transactions on Industrial Electronics*, vol. 66, no. 4, pp. 3139–3147, 2018.

[23] L. Zhang and H. Gao, "Asynchronously switched control of switched linear systems with average dwell time," *Automatica*, vol. 46, no. 5, pp. 953–958, 2010.

[24] J. Zhang, M. Li, and R. Zhang, "New computation method for average dwell time of general switched systems and positive switched systems," *IET Control Theory & Applications*, vol. 12, no. 16, pp. 2263–2268, 2018.

[25] R. Sanfelice, D. Copp, and P. Nanez, "A toolbox for simulation of hybrid systems in matlab/simulink: Hybrid equations (hyeq) toolbox," in *Proceedings of the 16th international conference on Hybrid systems: computation and control*, 2013, pp. 101–106.